JOURNAL OF AGRICULTURAL AND FOOD CHEMISTRY

pubs.acs.org/JAFC Article

Detection, Structural Elucidation, and Biological Effects of Diverse *N*-Acyl-homoserine Lactone Signaling Molecules in the Plant-Promoting Endophytic Bacterium *Rhizobium oryzihabitans* M15

Juanjuan Zhao, Guomin Ai, Sheng Yang, Xiaoxia Zhang,* and Guishan Zhang*

Cite This: *J. Agric. Food Chem.* 2021, 69, 9693−9705 Read Online

ACCESS | Metrics & More | Article Recommendations | Supporting Information

ABSTRACT: Quorum sensing (QS), usually performed by *N*-acyl-homoserine lactones (AHLs) in Gram-staining-negative bacteria, plays an important role in plant−bacteria interactions. *Rhizobium oryzihabitans* M15 is a plant-growth-promoting rhizobacterium (PGPR) isolated from rice roots. In this study, we found a QS system in the endogenous plasmid of *R. oryzihabitans* M15 and detected the activity of AHLs by a bioassay method. We identified five AHL analogues in *R. oryzihabitans* M15 using liquid chromatography-tandem mass spectrometry (LC-MS). The most dominant AHL analogue was *N*-(3R-hydroxy-7-*cis*-tetradecanoyl)-L-homoserine lactone according to nuclear magnetic resonance (NMR) and Mosher's reactions. Furthermore, the *rosI* mutant abolished AHL production and significantly decreased growth, exopolysaccharide (EPS) production, biofilm formation, and motility compared to the wild-type strain. These results lay the foundation for further investigating the QS regulation mechanism and signal pathway of *R. oryzihabitans* M15 and its interactions with the host plant.

KEYWORDS: *N-acyl-homoserine lactones (AHLs), structural elucidation, biofilm formation, exopolysaccharides, motility, growth rate*

Downloaded via CHINESE ACADEMY AGRICULTURAL SCI on December 30, 2021 at 02:55:54 (UTC).
See https://pubs.acs.org/sharingguidelines for options on how to legitimately share published articles.

INTRODUCTION

Quorum sensing (QS) is a cell-to-cell communication process that enables bacteria to orchestrate collective behaviors in response to changes in the cell density and species composition of the vicinal community.[1] This process involves the production, secretion, accumulation, and recognition of small diffusible signaling molecules called autoinducers (AIs).[2] *N*-Acyl-homoserine lactones (AHLs) represent a group of well-studied AIs in Gram-staining-negative bacteria. AHLs share a common skeleton, a homoserine lactone ring with an acyl side group. The diversity and specificity of AHLs are based on the number of carbon atoms (4−18) on the acyl chain, the substituent (hydrogen, oxhydryl, or carbonyl) present on the third carbon atom, and the degree of unsaturation. The identification of AHLs is most commonly performed by thin-layer chromatography (TLC) or liquid chromatography-tandem mass spectrometry (LC-MS/MS). Nevertheless, identification is usually hampered by limited AHL standards. Structural elucidation of unknown AHLs requires a sufficient number of molecules to support chromatographic and structural analyses. However, AHLs are generally present in culture media at nanomolar concentrations or less; thus, their identification by chemical methods is very challenging.[3]

Rhizobia are some of the best-studied plant-associated bacteria for investigating interactions and colonization.[4] QS is involved in the regulation of genes specific for rhizobial survival, as well as symbiosis or interactions, such as growth, exopolysaccharide (EPS) production, nodulation or nitrogen fixation, motility, and biofilm formation.[5] The first AHL identified in *Rhizobium* spp. was *N*-3-hydroxytetradecenoyl-L-homoserine lactone (3-OH, $C_{14:1}$-HSL), which is produced by *Rhizobium leguminosarum* and functions in growth inhibition, EPS cleavage regulation, and biofilm formation.[5,6] However, this AHL has not been found in other bacteria, including rhizobia, until now. QS regulatory systems in rhizobia are highly diverse, and even the same QS system in different species often regulates distinct functions. For example, in *R. leguminosarum*, the *cinI*/*R*-based QS system influences the synthesis of other AHLs as well as plasmid transfer.[7] However, in *Rhizobium etli*, the *cinI*/*R*-based QS system was shown to be expressed during symbiosis and to be involved in bacteroid development and symbiotic nitrogen fixation.[8] QS has also been detected in some phytopathogenic species; for example, *Agrobacterium vitis* produces six AHLs involved in swarming and plant−bacteria interaction regulation.[9,10] Despite the ubiquity of QS systems in *Rhizobium* spp., QS has rarely been identified and functionally elucidated in nonlegume plant-promoting endophytic bacteria, especially which are incapable of nitrogen fixation.

Plant-growth-promoting rhizobacteria (PGPR) have been widely used in agriculture for their environmentally safe and plant-growth-promoting properties.[11] *Rhizobium oryzihabitans* M15 is a novel PGPR isolated from rice roots in our previous work.[12] The vast majority of strains in the *Rhizobium* genus have the ability to nodulate and fix nitrogen. However, despite being classified as the *Rhizobium* genus, no nodulation- or

Received: June 29, 2021
Revised: July 30, 2021
Accepted: August 3, 2021
Published: August 17, 2021

ACS Publications © 2021 American Chemical Society

nitrogen-fixation-related genes were found in the complete M15 strain genome[12] (accession number: SAMN14048699). Numerous *Rhizobium* spp., without the function of nodulation or nitrogen fixation, have been isolated from nonlegume plants in recent years, some of which can colonize the rhizosphere well and enhance plant growth or induce plant resistance, such as *Rhizobium wuzhouense*,[13] *Rhizobium radiobacter* F4,[14,15] and *Rhizobium oryzicola*.[16] However, there is rare further research on these bacteria. Furthermore, strain M15 was closely related to *R. radiobacter* in taxonomy, most of which are phytopathogenic organisms causing crown gall disease across thousands of different plant species.[17] However, we did not find a VirB IV secretion system in *R. oryzihabitans* M15, a major virulence determinant causing crown gall disease in *R. radiobacter*.[12,18,19] There was also no pathogenicity after rice inoculation. In summary, *R. oryzihabitans* M15 represents a novel nonlegume species that requires further study.

In this study, a LuxI-/LuxR-like QS system was found in *R. oryzihabitans* M15, and a LuxI homologue located on endogenous plasmid was shown to encode AHL synthase based on its complete genome sequences, which synthesized at least five AHL molecules. We elucidated the structures of the AHL analogues. In addition, the AHL synthase-encoding gene was deleted. This mutant abolished the production of the five AHLs and was assessed to determine whether the QS system regulated the bacterial processes related to bacterial survival and colonization, including growth rate, biofilm formation, EPS production, and motility in *R. oryzihabitans* M15.

MATERIALS AND METHODS

Chemicals and Reagents. AHL standards were obtained from Sigma-Aldrich (St. Louis, MO) and Cayman Chemical (Ann Arbor, MI). Stock solutions of the analytes were prepared in acetonitrile (CH_3CN) and preserved at 4 °C. (*S*)-Methoxy-2-(trifluoromethyl) phenylacetyl chloride [(*S*)-MTPA-Cl] and (*R*)-methoxy-2-(trifluoromethyl) phenylacetyl chloride [(*R*)-MTPA-Cl] were purchased from Sigma-Aldrich (St. Louis). Silica gel was obtained from Qingdao Marine (Qingdao, China). Chromatographic-grade acetonitrile and formic acid were supplied by Merck (Darmstadt, Germany). Ultrapure water was prepared using a Milli-Q water purification system (Millipore Corp. Bedford, MA).

Bacterial Strains and Culture Conditions. *R. oryzihabitans* M15 (Deposit no. ACCC 60121) was identified as a novel PGPR strain in our previous work[12] and was cultured in Luria−Bertani (LB), yeast extract mannitol broth (YMA), and tryptone yeast extract (TY) at 30 °C. The AHL synthase gene in-frame mutant of *R. oryzihabitans* M15 was obtained by the traditional homologous recombination method and used to evaluate the bacterial physiological process regulated by QS. *Chromobacterium violaceum* CV026 and *Agrobacterium tumefaciens* NTL4 (pZLR4) were grown at 28 °C in LB and Agrobacterium minimal (ABM) media, respectively.

Detection of AHL Activities. AHL activities of *R. oryzihabitans* M15 were detected using *C. violaceum* CV026 and *A. tumefaciens* NTL4 (pZLR4) biosensor strains. Briefly, 5 μL of the tested sample extraction was spotted onto agar containing *C. violaceum* CV026, *A. tumefaciens* NTL4, and 40 μg/mL 5-bromo-3-chloro-3-indoly-1-β-D-galactopyranoside (X-gal). The plates were incubated at 28 °C for 12−48 h. In addition, AHL standards (C_6-HSL and C_8-oxo-HSL) were included as a positive control. Cell-free media extraction was used as a negative control.

Identification and Sequence Analysis of LuxI/LuxR Homologues. Whole-genome sequences were used to detect the QS system in *R. oryzihabitans* M15. The deduced amino acid sequence identity of LuxI/LuxR homologues obtained from *R. oryzihabitans* M15 was determined using NCBI (National Center for Biotechnology Information) BLASTP (protein basic local alignment search tool). Multiple sequence alignments of LuxI homologues in *R. oryzihabitans* M15 and other LuxI homologues were conducted using ClustalW (https://www.genome.jp/tools-bin/clustalw) and presented using ESPript 3.0 (http://espript.ibcp.fr/ESPript/). The sequences of LuxI homologues, including RmLuxI (*R. leguminosarum*), RiLuxI (*Rhizobium indigoferae*), RlLuxI (*Rhizobium laguerreae*), RpLuxI (*Rhizobium phaseoli*), ReLuxI (*R. etli*), RtLuxI (*Rhizobium aethiopicum*), AvLuxI (*Amblycerus vitis*), AtLuxI (*A. tumefaciens*), and RuLuxI (*Rhizobium pusense*), were obtained from the NCBI protein database. Phylogenetic trees were constructed using MEGA 7.0 software with the neighbor-joining method.

Extraction of AHLs for LC-MS Analysis and AHL Purification. *R. oryzihabitans* M15 was cultured in LB broth at 30 °C to the late exponential or early stationary phase (approximately 24 h). Bacterial cells were removed by centrifugation at 3200*g* for 20 min at 4 °C. Cell-free supernatant was extracted with an equal volume of acidified ethyl acetate (0.1% v/v glacial acetic acid) three times and dried using a rotatory evaporator at 30 °C. The residue was resuspended in acidified acetonitrile (0.1% formic acid; Merck, Germany) and stored at −20 °C. The prepared partial samples were filtered through a 0.45 μm Millipore filter prior to LC-MS analyses. Additionally, the remaining samples were subjected to purification.

Identification of AHLs by LC-MS. AHLs were identified by an Agilent 6460 Triple Quad LC-MS system (Agilent Technologies Inc., Santa Clara, CA). Separation was performed using a C_{18} reverse-phase column (2.1 mm × 100 mm, 3.5 μm particle size, Agilent ZORBAX SB-AQ, Agilent Technologies Inc., Santa Clara, CA). The column oven temperature was set to 30 °C. The mobile phase was composed of 2% acetonitrile in high-performance liquid chromatography (HPLC)-grade Milli-Q water (phase A) and pure acetonitrile (phase B). Separation was obtained using the following conditions: starting with 5% phase B and gradually increasing to 95% in 30 min at a flow rate of 0.25 mL/min. The injection volume was 5 μL.

Ionization was performed with an electrospray ionization (ESI) source in the positive mode. The probe capillary voltage was set at 4 kV, and the nebulizer pressure was set at 40 psi. For LC-MS analysis, the fragmentor voltages were set at both 95 and 165 V. For LC-MS/MS analysis, the collision energy and fragmentor voltages were set at 15 and 95 V, respectively.

Purification and Identification of AHLs. Structural elucidation of unknown AHL analogues was performed by chromatographic and structural analyses of pure AHL analogue solutions. The crude extract was separated by silica gel column chromatography, and the elution system was *n*-hexane/ethyl acetate (7:3, 5:5, 4:6, 3:7, 2:8, 1:9, 0:1 v/v, each 700 mL) and ethyl acetate/methanol (5:5, 3:7, 2:8, 1:9, 1:19, 0:1 v/v, each 700 mL); 13 fractions were obtained. The fractions obtained from silica gel column chromatography were tested for the presence of AHLs by a biosensor and confirmed by LC-MS. The activated fractions were purified by HPLC using a C_{18} reversed-phase column (ZORBAX SB_AQ, Agilent Technologies Inc., Santa Clara, CA; 4.6 mm × 150 mm, 5 μm particle size).

Pure AHLs were analyzed by nuclear magnetic resonance (NMR), and spectra were recorded in acetone on a Bruker 500 MHz NMR spectrometer (^{1}H: 500 MHz, ^{13}C: 126 MHz). Chemical shifts (δ) are reported as ppm based on the tetramethyl silane signal. Molecular weight and molecular formula were determined by high-resolution (HR)-ESI-MS using a Fourier transform ion cyclotron resonance mass spectrometer (Solarix XR). Absolute configuration was determined by high-field NMR Mosher's method. For the preparation of (*S*)- and (*R*)-MTPA esters of compounds, we used the procedures and chemical reactions detailed by Ohtani et al.[20]

Growth Rate Analysis. To confirm whether the *rosI* mutation affected the growth of *R. oryzihabitans* M15, the growth curves of the wild-type and *rosI* mutant strains were measured. A 5 mL culture of each strain was inoculated with a single colony and grown in LB medium at 30 °C overnight. Then, the cells were subcultured (1:100) into fresh LB, YMA, and TY media. The starting optical density at 600 nm (OD_{600}) of all tested strains was the same. Cell density was measured by monitoring the OD_{600} using a spectrophotometer at 2 h intervals. Triplicate experiments were performed in this manner.

https://doi.org/10.1021/acs.jafc.1c03895
J. Agric. Food Chem. 2021, 69, 9693−9705

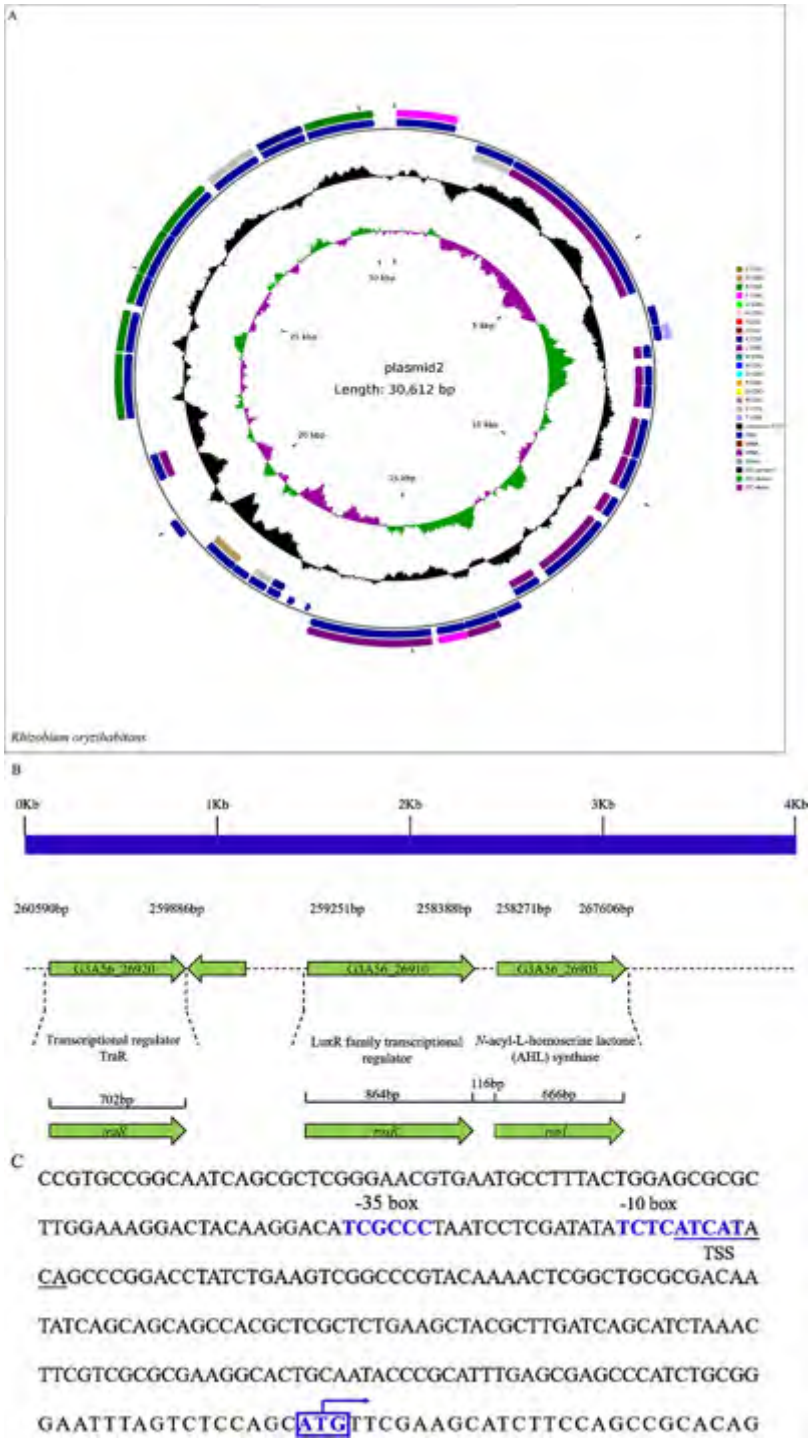

Figure 1. continued

https://doi.org/10.1021/acs.jafc.1c03895
J. Agric. Food Chem. 2021, 69, 9693−9705

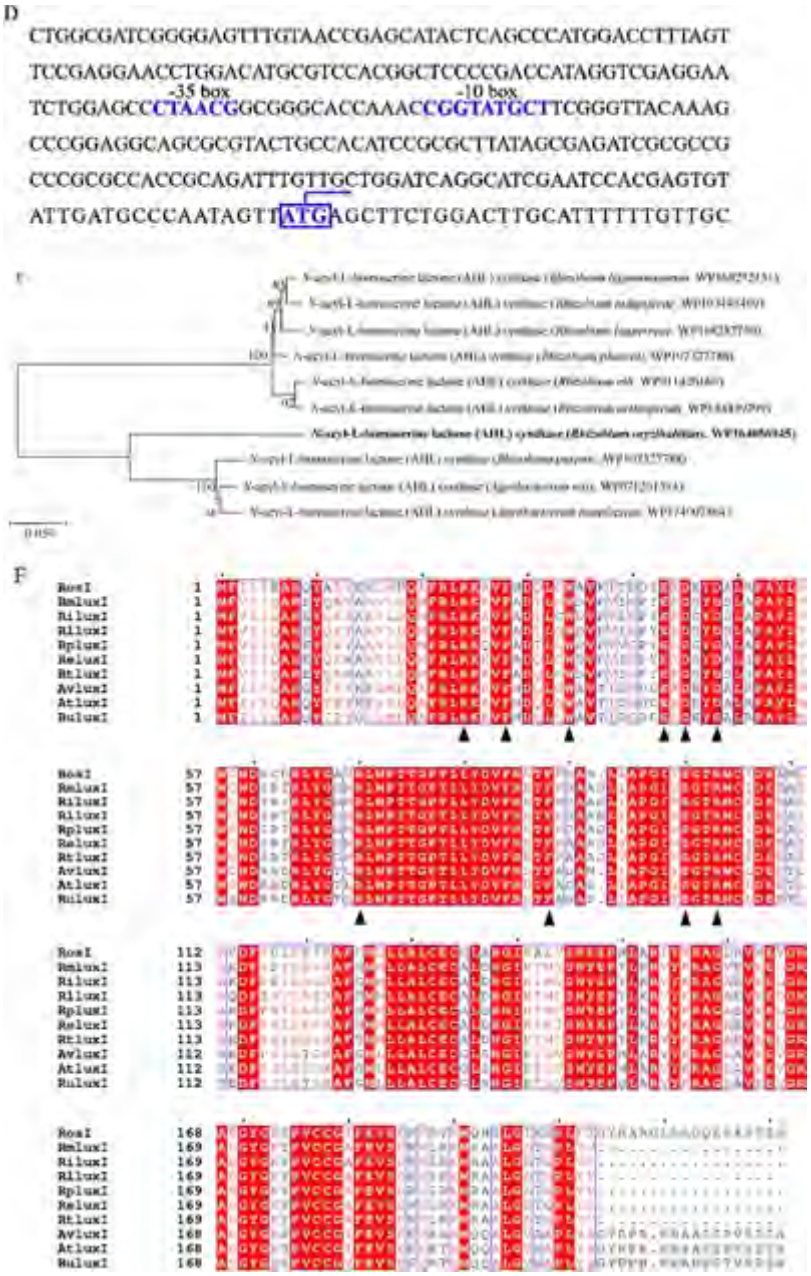

Figure 1. Genetic analysis of the QS system in *R. oryzihabitans* M15. (A) Genomic circle map of *R. oryzihabitans* M15 where the RosI/RosR are located. (B) Physical map of the QS system in *R. oryzihabitans* M15. Arrows represent the location and orientation of the genes. (C) Promoter sequence analysis of the *rosI* gene. (D) Promoter sequence analysis of the *rosR* gene. The putative -10 and -35 promoter sequences are in bold and blue color. The putative transcriptional regulator binding site (TSS) is denoted with an underscore. The predicted start codon is framed, and the arrow shows the orientation of transcription. (E) Phylogenetic tree of RosI against selected *N*-acyl-L-homoserine lactone (AHL) synthase from other *Rhizobium* species. The tree was constructed using the neighbor-joining algorithm with 1000 bootstrap values. Bar 0.050 indicates evolutionary distance. (F) Multiple sequence alignment of RosI with LuxI homologues: RmLuxI, RiLuxI, RlLuxI, RpLuxI, ReLuxI, RtLuxI, AvLuxI, AtLuxI, and RuLuxI (GenBank IDs: WP168272151, WP193445469, WP168287750, WP107327788, WP011426160, WP184459299, WP071201514, WP174007864, and WP107327788, respectively).

Biofilm Formation Assay. Biofilm formation was measured quantitatively by the crystal violet assay.[21] Briefly, logarithmic phase cells were used to inoculate LB, TY, and YMA broth media (starting OD_{600} of 0.05) and subpacked (10 mL) into wells of a 6-well plate without shaking. Biofilm formation was measured at 2, 3, and 4 days. For quantitative analysis, wells were washed twice with Milli-Q water and then stained with crystal violet (10 mL of a 1 wt %/vol crystal violet staining solution) for 20 min, rinsed with water to remove excess solution, and dried. Crystal violet bound to the wells was measured by dissolving it in 95% ethanol and measuring the OD_{570} nm with a Bio-Rad model 550 plate reader.

EPS Assay. EPSs were extracted from the *R. oryzihabitans* M15 cell culture fluid as described previously.[22] Total polysaccharides (expressed as μg/mL) of filtrate were quantified by anthrone-sulfuric acid with glucose as the standard. The steps were as follows: an appropriate amount of EPS solution (0.4 mL) was added to a clean glass test tube, and 0.1 mL of fresh 2% anthrone (dissolved in ethyl acetate) was added. The reaction was maintained for at least 10 min at 100 °C after slowly adding 1 mL of 98% sulfuric acid dropwise and sealing the tube with parafilm. The EPS content was measured as the OD_{620} nm in a cuvette.

https://doi.org/10.1021/acs.jafc.1c03895
J. Agric. Food Chem. 2021, 69, 9693−9705

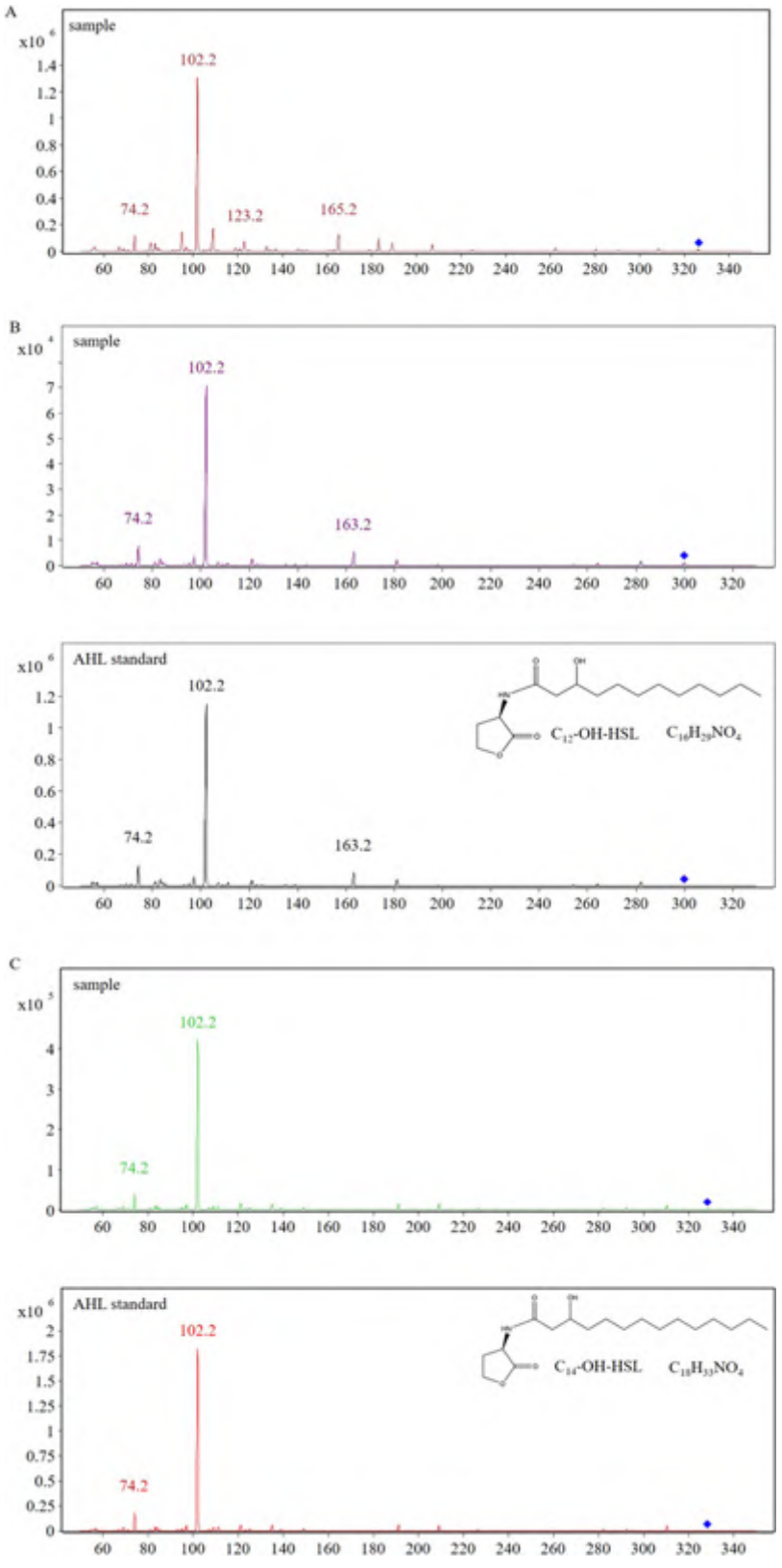

Figure 2. continued

https://doi.org/10.1021/acs.jafc.1c03895
J. Agric. Food Chem. 2021, 69, 9693−9705

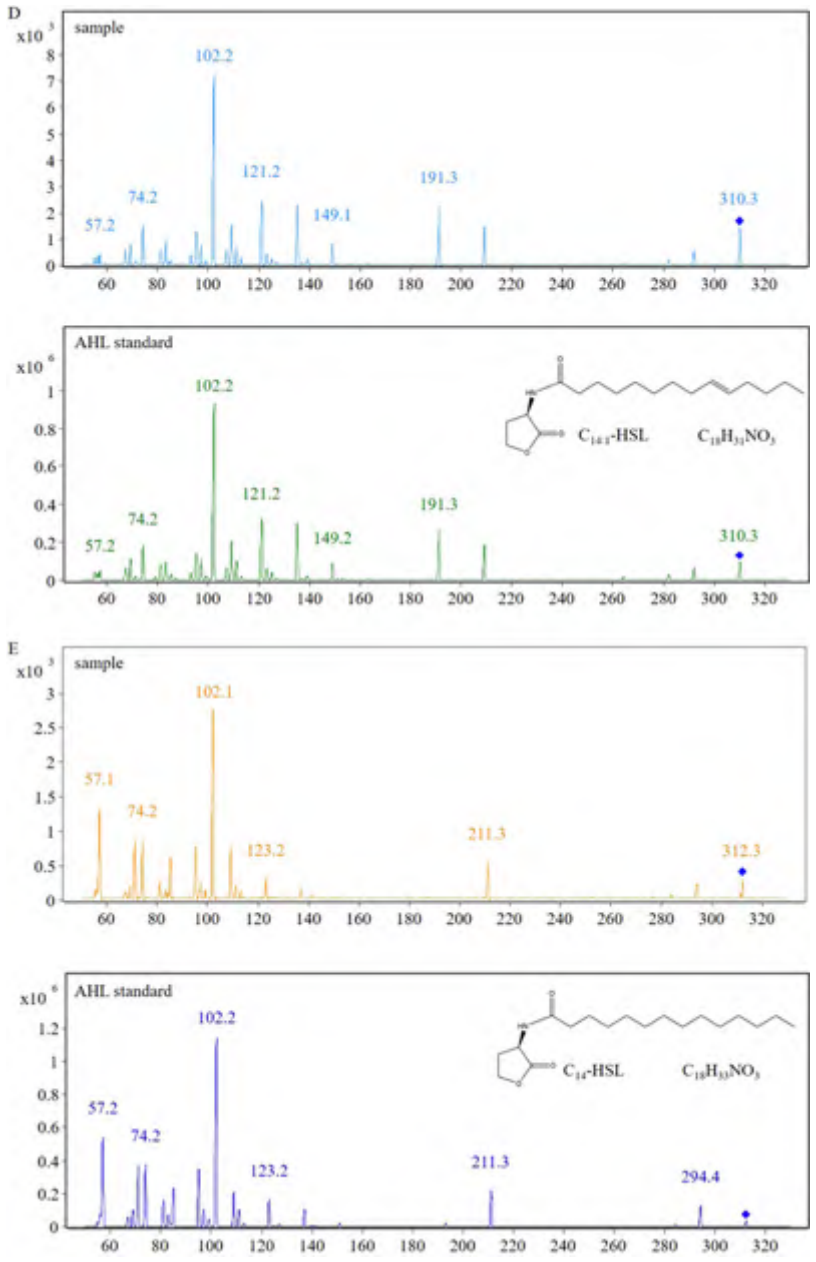

Figure 2. LC-MS ion chromatograms of AHLs produced by *R. oryzihabitans* M15 and AHL standards. (A) Mass spectrum obtained for the protonated molecules at *m*/*z* 326 of the sample prepared from the cultured medium of *R. oryzihabitans* M15. (B) Mass spectrum obtained for the protonated molecules at *m*/*z* 300 of the sample prepared from the cultured medium of *R. oryzihabitans* M15 (top one) and related AHL standard C12-OH-HSL (bottom one). (C) Mass spectrum obtained for the protonated molecules at *m*/*z* 328 of the sample prepared from the cultured medium of *R. oryzihabitans* M15 (top one) and related AHL standard C14-OH-HSL (bottom one). (D) Mass spectrum obtained for the protonated molecules at *m*/*z* 310 of the sample prepared from the cultured medium of *R. oryzihabitans* M15 (top one) and related AHL standard C14:1-HSL (bottom one). (E) Mass spectrum obtained for the protonated molecules at *m*/*z* 312 of the sample prepared from the cultured medium of *R. oryzihabitans* M15 (top one) and related AHL standard C14-HSL (bottom one). The structure and molecular formula of related AHL standard are placed at the top right of the mass spectrum.

Motility Assay. Bacterial motility was assessed on 1/10 TY plates containing 0.3 and 0.75% agar for swimming and swarming assays, respectively.[23] An overnight culture of the corresponding strain to be analyzed was adjusted to identical cell density, and 2.5 μL of the sample was inoculated in the plate symmetrically and incubated at 30 °C. The movement was monitored for up to 24 h by measuring the hole diameter.

Statistical Analysis. Triplicate samples were utilized for each sample group, and all experiments were conducted in triplicate. Statistical analysis was performed using Origin software (OriginLab Corp., Northampton, MA). The data are expressed as the mean ± standard deviation (SD). The *t*-test was carried out to conduct the statistical analysis using one-way analysis of variance (ANOVA) using IBM SPSS Statistics 25 software. A $p < 0.05$ was considered to be significant.

RESULTS

Identification and Sequence Analysis of LuxI/LuxR Homologues in *R. oryzihabitans* M15. To mine QS systems, homologues of one luxI and six luxR of *R. oryzihabitans* M15 were found based on genome annotation

https://doi.org/10.1021/acs.jafc.1c03895
J. Agric. Food Chem. 2021, 69, 9693−9705

and the homologous protein Blast. The LuxI homologue was located on a 30, 612 bp endogenous plasmid (accession number: CP048637; Figure 1A), which was named *rosI* (*Rhizobiumoryzihabitans*). RosI encodes an AHL synthase of 221 amino acids with a molecular mass of 24.92 kDa. The deduced protein showed high similarity to members of the LuxI family, with 77.4% identity to that of the plant pathogen *Agrobacterium vitis*, which can produce at least six AHLs (C_6-HL, C_8-HL, 3-O-C_8-HL, $C_{14:1}$-HL, $C_{16:1}$-HL, 3-O-$C_{16:1}$-HL) and regulate the hypersensitive-like response (HR) and necrosis.[24] The deduced protein also shared 76.0% of the identity of that in *A. tumefaciens*, 75.0% of that in *R. pusense*, and more than 60.0% of that in some other bacteria of the genus *Rhizobium*. Phylogenetic analysis of LuxI family proteins further demonstrated that RosI was clustered together with the other LuxI homologues but formed a separated branch between LuxI homologues from *Rhizobium* and *Agrobacterium* (Figure 1E), which indicated that RosI belonged to the luxI family, but it also has its particularity. Additionally, the RosI protein of *R. oryzihabitans* M15 had 114 conserved residues with nine other LuxI-type AHL synthases from rhizobia, which contained all 10 highly conserved amino acids among LuxI homologues (Figure 1F). The *rosI* gene was preceded by a putative promoter at −35 (TCGCCC) and −10 (TCTCAT-CAT) and a potential transcriptional regulator binding site ATCATACA (Figure 1C).

A total of 6 LuxR homologues, namely, RosR (G3A56_26910), RosR2 (G3A56_RS14500), RosR3 (G3A56_07545), RosR4 (CFBP6625_00845), RosR5 (G3A56_08455), and TraR (G3A56_26920), were detected in *R. oryzihabitans* M15. The *rosR* gene was genetically linked to the *rosI* gene and located 116 bp upstream of the *rosI* gene (Figure 1B), while the *rosR2*, *rosR3*, and *rosR4* genes were located on the chromosome. The *traR* gene was located 1615 bp upstream of the *rosI* gene. Therefore, the *rosR* gene was further analyzed and shown to encode a LuxR family transcriptional regulator of 288 amino acids with a molecular mass of 32.01 kDa. The deduced rosR protein showed high similarity to members of the LuxR family, with 70.8% similarity to that in *R. pusense*, 70.3% similarity to TraR in *A. tumefaciens*, and more than 60.0% similarity to that in some other bacteria of the genus *Rhizobium*. Phylogenetic trees of RosR family proteins demonstrated that RosR was clustered together with the other LuxR homologues but formed a separated branch with RosR2, RosR3, RosR4, RosR5, and TraR. RosR2, RosR3, RosR4, and RosR5 were clustered together in one branch, and TraR was clustered in another separated branch (Figure S10). The results indicated that RosR had low homology with the other five luxR homologues in strain M15. The *rosR* gene was preceded by a putative promoter at -35 (CTAACG) and -10 (CGGTATGCT). However, no obvious transcriptional regulator binding sites were found in the region upstream of *rosR* (Figure 1D).

Detection of the Activity of AHL Analogues in *R. oryzihabitans* M15. AHL analogues were detected using *C. violaceum* CV026 and *A. tumefaciens* NTL4 (pZLR4) as bioreporters. The CviR of *C. violaceum* CV026 regulates the production of violacein when induced by short-chain AHLs.[25] *A. tumefaciens* NTL4 carries the plasmid pZLR4 containing a *traG*::*lacZ* fusion and *traR*, which produces a blue color by degrading X-gal in response to long-chain AHLs. Negative results of *C. violaceum* CV026 and positive results of the *A. tumefaciens* NTL4 bioassay indicated that *R. oryzihabitans* M15 can synthesize long-chain AHL analogues but not short-chain AHL analogues (Figure S1).

Identification of AHL Analogues by LC-MS and LC-MS/MS. LC-MS analyses were performed to screen the AHL analogues produced by *R. oryzihabitans* M15. The suspected AHL analogues could be found based on the in-source fragment ions m/z 102 and m/z 74 originating from the lactone ring of AHLs. Five AHL analogues ($[M + H]^+$) with m/z values of 300.3, 310.3, 312.4, 326.3, and 328.4, all of which gave the in-source fragment ion at m/z 102 (and m/z 74), were found (Figure S5). Three of these analogues (m/z 300.3, 326.3, and 328.4) were found from crude extraction. The ion at m/z 310.3 was detected from silica column fractions, and that at m/z 312.4 was detected from HPLC fractions.

Four AHL analogues (m/z 300.3, 310.3, 312.4, and 328.4) were further identified by LC-MS/MS analyses. The chromatographic retention times and mass spectral fragmentation pattern of the culture supernatant were the same as those of the synthetic AHL standards (Figure 2B−E, Table S1, Figure S5). The four compounds were determined to be C_{12}-OH-HSL, $C_{14:1}$-HSL, C_{14}-HSL, and C_{14}-OH-HSL, and their molecular formulas were assigned to be $C_{16}H_{29}NO_4$, $C_{18}H_{32}NO_4$, $C_{18}H_{31}NO_3$, and $C_{18}H_{33}NO_3$, respectively, with molecular weights of 299.41, 309.44, 311.46, and 327.46. The suspected AHL analogue with an m/z of 326.3 (named AHL analogue **1**) could not be identified by the standards and was further purified and identified as follows.

Purification and Characterization of AHL Analogue 1 in *R. oryzihabitans* M15. To identify AHL analogue **1**, we grew a large-volume *R. oryzihabitans* M15 culture and extracted it with ethyl acetate. The extract was separated using silica gel column chromatography and reversed-phase semipreparative HPLC and analyzed at 210 nm. Then, the activity was tested with the *A. tumefaciens* NTL4 indicator. Pure compounds were analyzed by HR-ESI-MS, NMR, and Mosher's reaction to identify the structure.

The molecular formula of AHL analogue **1** was characterized to be $C_{18}H_{31}NO_4$ (four unsaturation degrees) by its HR-ESI mass spectrum (m/z 326.23857 $[M + H]^+$, calcd 326.238572). The planar structure of AHL analogue **1** was determined by NMR spectra, including ^1H, ^{13}C, correlation spectroscopy (COSY), heteronuclear single quantum coherence (HSQC), and heteronuclear multiple bond correlation (HMBC) NMR spectra (Table 1, Figure S2), and the absolute configuration was established by modified Mosher's reactions. The proton signals at 1.28−1.35 ppm are the diagnostic characteristics of aliphatic chains, and the multiplets at 5.37 ppm implied that AHL analogue **1** contained a double bond. The $^1H-^1H$ COSY correlations gave three isolated proton spin systems corresponding to CH_2-2 to Me-14 and -*N*H-C-3′-C-4′-C-5′. The HMBC correlations from H-3, CH_2-2, and H-3′ to C-1 confirmed that C-1 was connected with C-2, and an amide bond was formed between C-3′ and C-1. The HMBC correlations from H-3′, CH_2-4′, and CH_2-5′ to C-2′ established a lactone ring system (Figure S7). Thus, the planar structure of **1** was characterized (Figure S7). The stereochemistry of C-3 was determined by the modified Mosher's reaction. Reactions of **1** with (*S*)-MTPA-Cl and (*R*)-MTPA-Cl formed the corresponding *R*-MTPA ester (**1a**) and *S*-MTPA ester (**1b**), respectively. The difference in chemical shifts ($\Delta\delta_{SR} = \delta_S - \delta_R$) for **1b** and **1a** established that the C-3 location had the *R* configuration (Table 1, Figure S8).

https://doi.org/10.1021/acs.jafc.1c03895
J. Agric. Food Chem. 2021, 69, 9693−9705

Table 1. NMR Data of Compound 1 in Actone-d_6 (δ in ppm and J in Hz) and Mosher's Reaction of Compound 1 in Actone-d_6 (δ in ppm and J in Hz)

	1		Mosher's reaction (1)	
position	^{1}H	^{13}C	^{1}H	^{13}C
1		172.9		172.9
2	2.31; 2.40	43.7	2.31; 2.39	43.7
3	3.94	68.9	3.93	69
4	1.48	37.5	1.47; 1.51	37.5
5	1.40;1.52	26.5	1.42;1.55	26.5
6	2.05	27.9	2.05	27.8
7	5.37	130.8	5.37	130.8
8	5.37	130.6	5.37	130.6
9	2.05	27.8	2.05	27.9
10	1.30	29.5	1.30	29.7
11	1.30	30.5	1.35; 1.29	30.5
12	1.28	32.6	1.30	32.5
13	1.30	23.4	1.30	23.4
14	0.88	14.4	0.88	14.4
NH	7.65		7.66	
2′		175.6		175.6
3′	4.66	49.2	4.67	49.2
4′	2.27; 2.59	29.6	2.27; 2.59	29.9
5′	4.29; 4.40	66.2	4.29; 4.40	66.2

rosI Mutant No Longer Synthesizes AHLs. To further understand the role of the QS system in *R. oryzihabitans* M15, the AHL synthase gene mutant (Δ*rosI*) strain was constructed by allelic exchange. The *rosI* gene was successfully deleted by the suicide plasmid pCM351. Polymerase chain reaction (PCR) in Δ*rosI* generated an 800 bp fragment, as expected, while a normal 1460 bp DNA fragment was amplified in the wild-type strain (Figure S11). The sequencing of PCR products confirmed that Δ*rosI* was successfully achieved.

The AHL activity of the *rosI* mutant was determined by *A. tumefaciens* NTL4 as a reporter strain and LC in the multiple reaction monitoring mode (MRM) using precursor ions of m/z 300.1, 326.1, 328.1, 310.1, and 312.1 and the same product ion of m/z 102. The negative result of the *A. tumefaciens* NTL4 bioassay indicates the abolishment of the AHL synthesis ability in *rosI* mutant (Figure S13). As shown in Figure S14, five AHLs, C_{12}-OH-HSL (m/z 300), $C_{14:1}$-OH-HSL (m/z 326), C_{14}-OH-HSL (m/z 328), $C_{14:1}$-HSL (m/z 310), and C_{14}-HSL (m/z 312), were identified in the supernatant extracts of the wild-type strain, while none of them were detected in the *rosI* mutant strain, which confirmed that the *rosI* gene was responsible for synthesizing five AHLs and that the *rosI* mutant strain abolished the AHL synthesis ability.

Quorum-Sensing Promotes _R. oryzihabitans_ M15 Growth. The growth rate in selective medium (YMA) and complete media (TY, LB) was determined. As shown in Figure S12, the growth of the *rosI* mutant declined compared to that of the wild-type strain in all tested media. The difference is mainly manifested in the delay to enter the exponential phase. The *rosI* mutant strain arrived at the exponential phase with a 10 h delay in the YMA medium. Additionally, there was only a 2-h delay in LB and TY media. However, no significant difference in the growth rate was observed during the exponential phase. We speculated that the abundant nutrients in the complete media might compensate for the growth defect of the mutant strain. It was concluded that QS positively regulated the growth of *R. oryzihabitans* M15 and that the regulation was more obvious in selective media than in complete media.

QS Increases Biofilm Formation in _R. oryzihabitans_ M15. The ability of rhizobia to establish the biofilm can be used as a strategy for survival or colonization and/or interaction. To determine the roles of QS and nutritional conditions in *R. oryzihabitans* M15 biofilm formation, both wild-type and *rosI* mutant strains were cultured in YMA, TY, and LB media. After 2, 3, and 4 days, the biofilm biomass was evaluated by crystal violet staining (Figure 3).

The biofilms formed by *R. oryzihabitans* M15 varied greatly in different media. In both wild-type and *rosI* mutant strains, the biofilm biomass increased with the extent of incubation time in all tested media. Biofilm formation in LB media was extremely obvious at 48 h, with biomasses of 10.7 and 8.4 (OD_{570} nm) for the wild-type and *rosI* mutant strains, respectively. With the extension of incubation time, although the biofilm biomass increased gradually in LB medium, it increased for the wild-type and *rosI* mutant strains by approximately 22.1 and 44.6% on the third day and 39.6 and 29.7% on the fourth day, respectively. Moreover, the formed biofilm was thick and uniform in the LB medium. However, in the TY medium, the biofilm was relatively thin and had a lower biomass in both the wild-type and *rosI* mutant strains. For example, when cultured for 4 days, the biomass of the wild-type and *rosI* mutant strains in the TY medium was 9.2 and 5.1 (OD_{570} nm), respectively, which was less than that in the LB medium after 2 days. Biofilm formation was much slower in the YMA medium; biofilms began to significantly form after 3−4 days, and the biomass of the wild-type strain increased by 205% compared with that of the *rosI* mutant strain. However, the YMA medium did not seem to be conducive to biofilm formation of the *rosI* mutant strain, the biomass of which was only 1.78 (OD_{570} nm) on the fourth day. We suspected that the nutrients in the media, especially the carbon source, are the major factors affecting the biofilm formation of *R. oryzihabitans* M15.

Predominantly, the biofilm formed in the *rosI* mutant was significantly impaired and decreased in all tested media compared to that in the wild-type strain. As shown in Figure 3, the *rosI* mutant had a significantly different total biofilm biomass in the LB medium compared to that of the wild-type strain M15 ($p < 0.05$) although the biofilm architecture and thickness of the biofilms were very similar. The total biofilm biomass of the *rosI* mutant in the LB medium decreased by approximately 21.0, 6.4, and 13.0% compared with that of the wild type on days 2, 3, and 4, respectively. However, no significant difference was observed in biofilms formed by wild-type and *rosI* mutant strains until day 3 in the TY medium. The biofilm of the *rosI* mutant was significantly thinner than that of the wild-type strain after 3 days, with decreases of 22.2 and 44.3% in biomass ($p < 0.01$). Wild-type biofilms were obviously thicker than those of the *rosI* mutant upon visual inspection in the YMA medium. Simultaneously, the biofilm biomass of the *rosI* mutant was significantly decreased by approximately 79.0, 77.0, and 90.8% on days 2, 3, and 4, respectively ($p < 0.01$). In summary, the results revealed that QS positively regulated the biofilm formation of *R. oryzihabitans* M15. Biofilm formation is a complex process, and the effect of QS on biofilms can be nutritionally conditional.[26]

QS Affects EPS Production in _R. oryzihabitans_ M15. In some *Rhizobium* strains, QS is necessary for the synthesis of

https://doi.org/10.1021/acs.jafc.1c03895
J. Agric. Food Chem. 2021, 69, 9693−9705

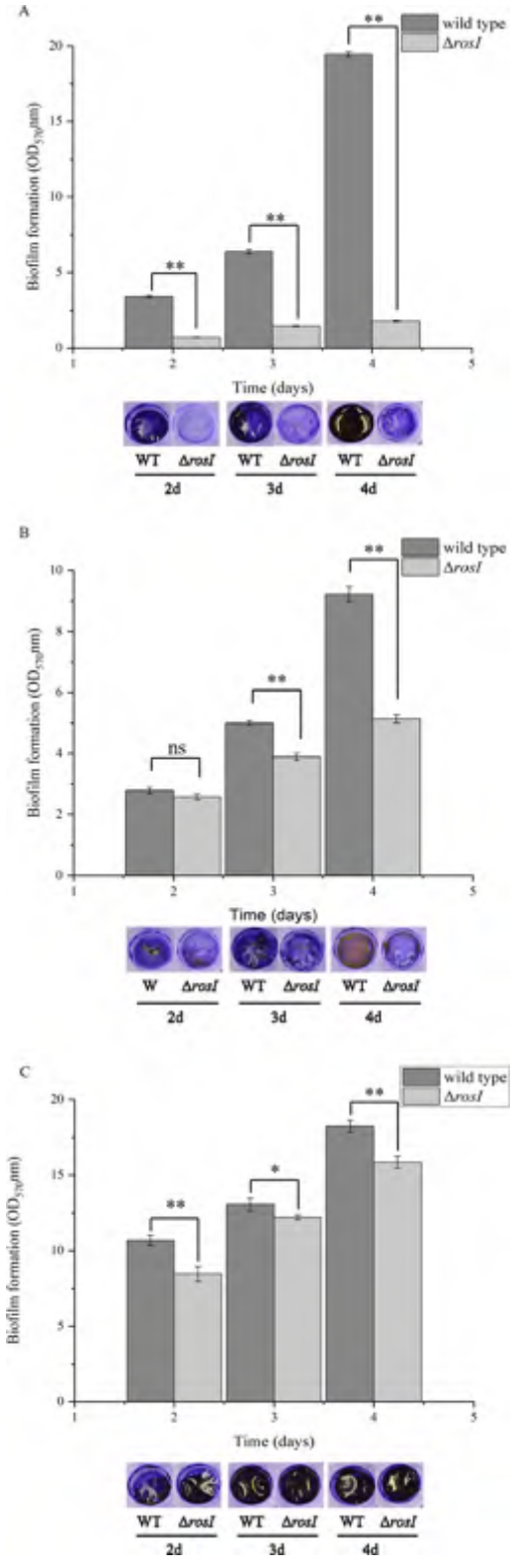

Figure 3. Effect of quorum sensing on biofilm formation of *R. oryzihabitans* M15. (A) The strains (wild-type and *rosI* mutant) were allowed to form a biofilm in YMA media at 30 °C for 4 days. (B) The strains were allowed to form a biofilm in TY media at 30 °C for 4 days. (C) The strains were allowed to form a biofilm in LB media at 30 °C for 4 days. The formed biofilms were stained with crystal violet and quantified by measuring the absorbance at 570 nm. The error bars represent the standard deviation of biological triplicates. *p < 0.05, **p < 0.01.

symbiotically important EPSs. In this work, we assessed whether QS had similar regulatory functions in nonsymbiotic *R. oryzihabitans* M15. The wild-type and *rosI* mutant strains were investigated for the production of EPSs. Our results showed that inactivation of the *rosI* gene resulted in a significant decrease in EPS production (p < 0.01) in the three tested media (Figure 4). In the YMA medium, the EPS concentrations of the wild-type strain were 507.2 ± 15.5, 658.8 ± 17.1, and 1177.8 ± 43.2 μg/mL at 28, 34, and 40 h, respectively. However, for the *rosI* mutant strain, the EPS concentrations were 138.4 ± 7.2, 353.7 ± 30.7, and 607.4 ± 26.8 μg/mL at 28, 34, and 40 h, which was decreased by 72.7, 46.3, and 48.4% compared to that of the wild-type strain, respectively. For TY and LB media, although the EPS concentration of the *rosI* mutant strain was still significantly lower than that of the wild-type strain, the EPS concentration was much lower than that in the YMA medium, which was less than 100 μg/mL for both the wild-type and *rosI* mutant strains. Altogether, these results indicate that QS plays a critical role in the regulation of EPS production in *R. oryzihabitans* M15 and that the production of EPSs is also affected by culture conditions.

QS Affects Motility in *R. oryzihabitans* M15. Motility allows for rhizobia to find their specific host plant and establish interactions. QS has been shown to be involved in the regulation of various rhizosphere bacteria. Swimming and swarming motility data for both the wild-type and *rosI* mutant strains are presented in Figure 5. The *rosI* mutant strain exhibited significantly weakened swimming motility compared with the wild-type strain (p < 0.01) after 2 days of incubation. Compared to that of the wild-type strain, the swimming diameter decreased by 21.01% in the *rosI* mutant strain. However, the size of the spotted colony did not change on 0.75% agar plates in either the wild-type or *rosI* mutant strain after 7 days, indicating no swarming motility from the site of inoculation. These data suggested that QS is an important regulatory factor in the swimming motility of *R. oryzihabitans* M15.

DISCUSSION

Rhizobia, famous mutualistic symbiotic bacteria with nitrogen fixation, play a critical role in both plant ecosystems and sustainable agriculture. Strains of rhizobia that do not fix nitrogen or are not symbiotic are still common in the soil and nonlegume plants, including rice. QS is an important system that regulates specific functions in rhizobia. However, little is known regarding the production and structure of signaling molecules and mechanisms of communication among rice-related rhizobial strains.

In this study, we report the production of AHL signaling molecules by rice-associated *R. oryzihabitans* M15 for the first time, which were identified as $C_{14:1}$-OH-HSL, C_{12}-OH-HSL, $C_{14:1}$-HSL, C_{14}-HSL, and C_{14}-OH-HSL. Several studies have reported that some LuxI orthologues catalyze the synthesis of more than five AHLs. For example, *Bradyrhizobium* sp. SR-6 was reported to produce seven AHLs with C6-C12 chains substituted with hydrogen, carbonyl, or oxhydryl at 3′ carbons,[27] which differs from strain M15 in producing short-chain AHLs and 3′ oxo carbon AHLs. *Sinorhizobium meliloti* Rm1021 produced eight AHLs with 12−18 carbons in the acyl side chain.[5] Although both the Rm1021 and M15 strains produced long-chain AHLs, it is possible that they produce different types of AHL molecules. In strain Rm1021, the C-3

https://doi.org/10.1021/acs.jafc.1c03895
J. Agric. Food Chem. 2021, 69, 9693−9705

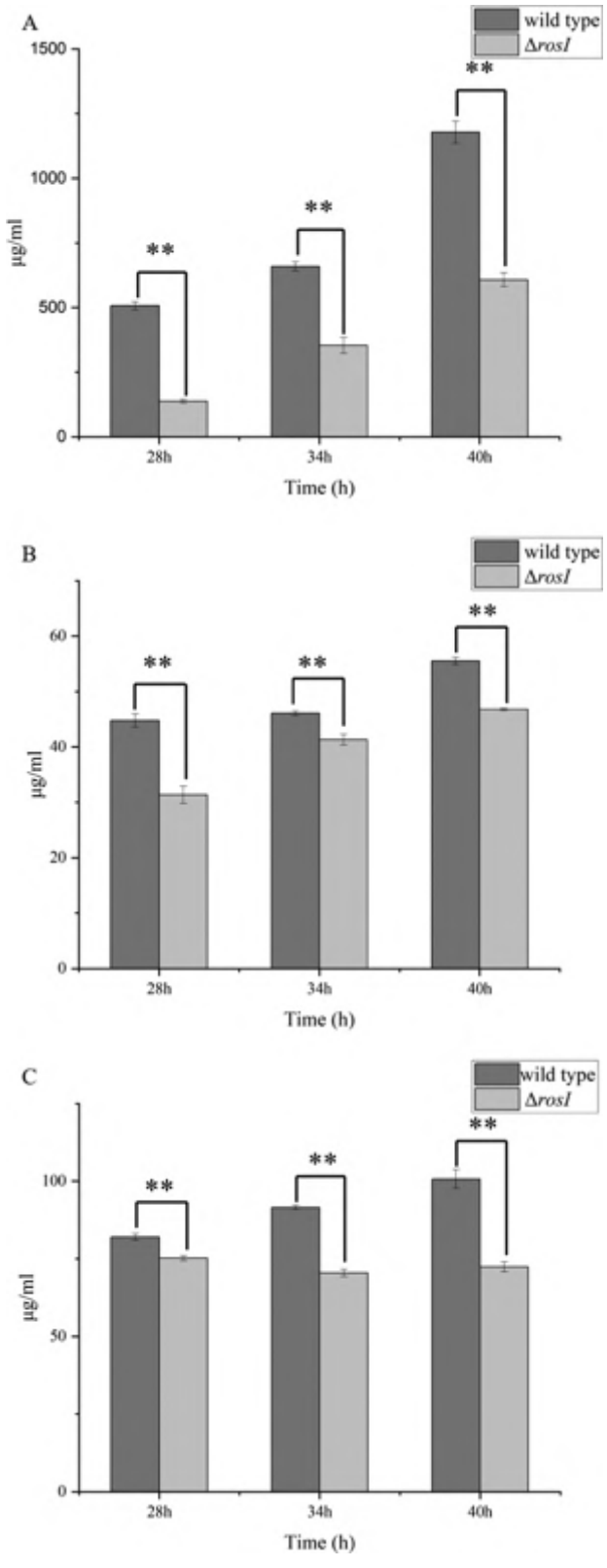

Figure 4. Effect of quorum sensing on EPS production by wild-type and *rosI* mutant (Δ*rosI*) of *R. oryzihabitans* M15. (A) EPS production in YMA media at 30 °C for 40 h. (B) EPS production in TY media at 30 °C for 40 h. (C) EPS production in LB media at 30 °C for 40 h. The values are the mean of three independent biological replicates. The error bars indicate mean ± standard deviation of three biological replicate determinations.

position of the AHL molecules is substituted by hydrogen or carbonyl. However, hydrogen or oxhydryl are substituted on the 3rd carbon atom of AHL molecules produced by strain M15. Therefore, the AHLs produced by the M15 strain were unique in structure. The structural diversity of AHLs depends on the differences in both substrate and gene structure and further determines the diversity of functional regulation.

$C_{14:1}$-OH-HSL is the major AHL produced by strain M15. Simultaneously, it is also produced by the legume-symbiotic rhizobia *R. leguminosarum*, in which it plays a role in the regulation of growth inhibition, plasmid transfer, EPS cleavage, and biofilm formation.[5] C_{12}-OH-HSL has also been identified in the *Bradyrhizobium* sp. strain SR-6, a soybean nodule endophytic bacterium, and regulated nodulation.[27] $C_{14:1}$-HSL was detected in *A. vitis*, a plant pathogen that participates in the regulation of the HR and causes necrosis.[28] C_{14}-HSL was identified in an aerobic granular sludge system and plays an important role in regulating LB-EPS and TB-EPS production;[29] likewise, this AHL was also found in wastewater treatment systems.[30] In many bacteria, such as ammonia-oxidizing bacteria (AOB), *Porphyromonas gingivalis*, *Pseudomonas fluorescens*, *Pseudomonas aeruginosa*, *Nitrosospira multiformis*, *Gluconacetobacter diazotrophicus* PAL5, and *Serratia liquefaciens* ATCC 27592, the presence of C_{14}-HSL has also been identified and was shown to inhibit growth in *P. gingivalis*, enhance the tolerance to drought in red rice plants in *G. diazotrophicus* PAL5, and enhance metabolic activity in AOB.[31−37] However, the functions of C_{14}-HSL in other bacteria remain to be further studied. The C_{14}-HSL signaling molecule was also detected in rhizobia; this AHL regulated biofilm formation in the *Sinorhizobium fredii* strain SMH12 but coregulated EPS production, surface translocation, motility, growth rate, and nodulation with other AHLs produced by *S. meliloti* Rm1021.[5] C_{14}-OH-HSL was detected in *Rhodospirillum rubrum* and *R. etli* RT1 and was shown to regulate swarming motility and biofilm formation.[5] Except for C_{14}-HSL, the other four AHLs produced by *R. oryzihabitans* M15 mainly existed in rhizobia. It is interesting that the QS signaling molecules of strain M15 are similar to those of legume-symbiotic nitrogen fixation rhizobia and possess the same AHL as pathogenic *Agrobacterium*. This should be consistent with the particularity of strain M15. This strain is similar to the pathogenic *Agrobacterium* but lacks pathogenicity-related genes in the genome; likewise, the strain is classified as *Rhizobium*, but nodulation- and nitrogen-fixation-related genes are missing in the genome. In this study, we clarified the structural diversity of AHLs produced by strain M15, a PGPR bacterium, which is an important basis for further research on its functional regulation and regulation mechanism interpretation.

Biofilm formation, regulated by QS in some rhizosphere bacteria, is affected by many nutritional and environmental conditions (such as extreme temperature or pH) and multivalent cations (Ca^{2+}, Cu^{2+}, Mg^{2+}, and Fe^{3+}).[38] In *S. meliloti*, nutrient sources enhance biofilm formation, while extreme conditions prevent biofilm formation.[39] When yeast extract or calcium was removed from the TY medium, *A. caulinodans* did not form biofilms.[38] Similarly, in this study, biofilm formation of *R. oryzihabitans* M15 was positively affected by QS. However, obvious biofilm formation was not observed by the *rosI* mutant in the YMA medium. This may be contributed by the significant delay of the growth rate in the YMA medium. Since the measurement of biofilm formation is static culture, the difference in growth rate is extremely

https://doi.org/10.1021/acs.jafc.1c03895
J. Agric. Food Chem. 2021, 69, 9693−9705

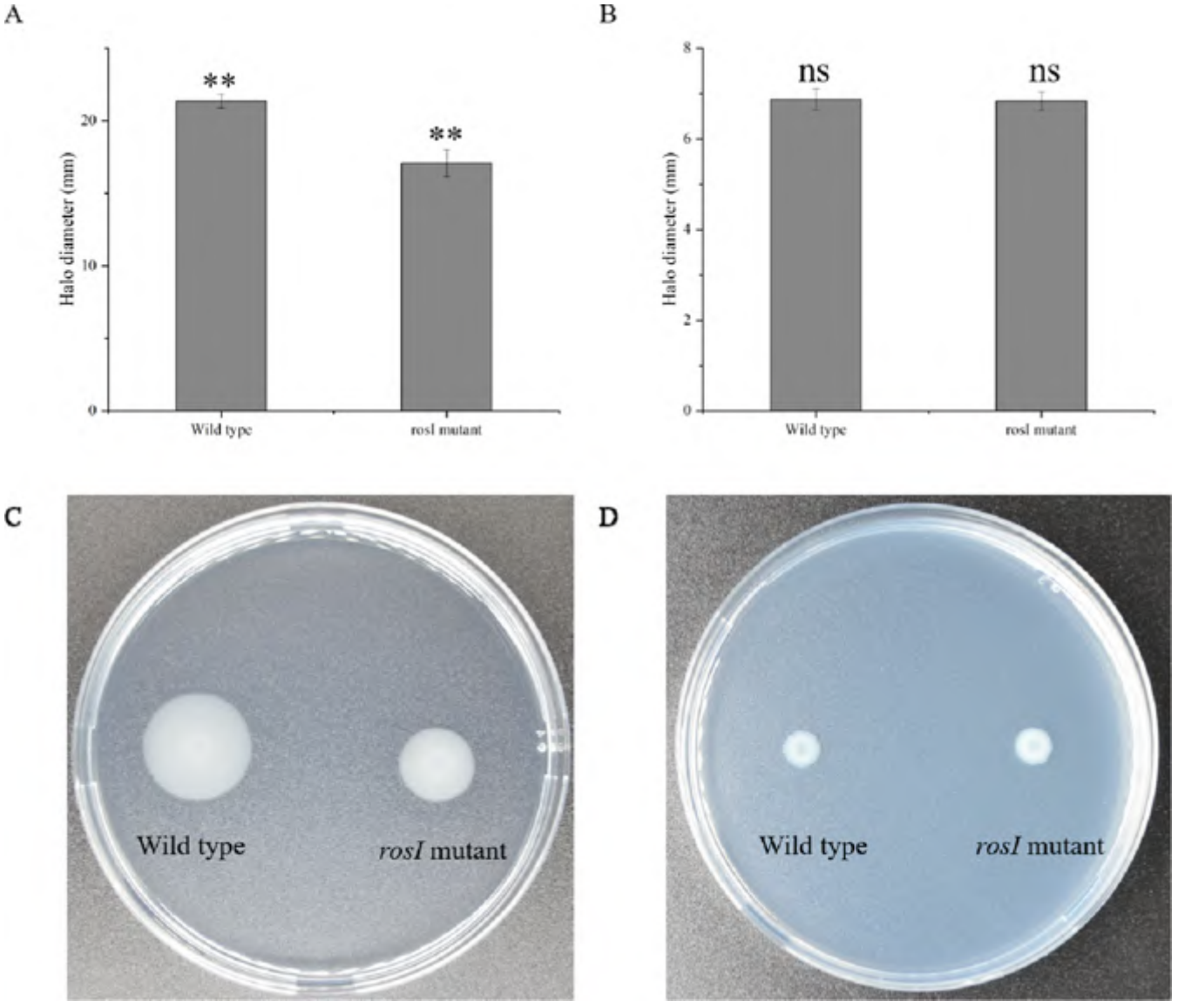

Figure 5. Motility of wild-type and *rosI* mutant strains of *R. oryzihabitans* M15. (A) Swimming diameter of wild-type and *rosI* mutant strains at 30 °C for 2 days. (B) Swarming diameter of wild-type and *rosI* mutant strains at 30 °C for 7 days. (C) Swimming motility of wild-type and *rosI* mutant strains inoculated onto the surface of 0.3% of 1/10 TY agar at 30 °C for 2 days. (D) Swarming motility of wild-type and *rosI* mutant strains inoculated onto the surface of 0.75% of 1/10 TY agar at 30 °C for 7 days. Data was mean ± SD of three independent experiments.

magnified compared to shaking conditions. Moreover, the difference in the biomass of biofilm formation in the nutrient-rich media (TY and LB) mentioned might be caused by the distinction in nutrition content (tryptone and yeast extract) and multivalent cations (Ca^{2+}). In rhizobacteria, flagella-mediated motility is essential for biofilm establishment and therefore for plant colonization and is regulated by QS.[40] For example, *S. meliloti* showed reduced biofilm formation ability in flagella synthesis-related gene mutants.[41] The results in this work indicate that the swimming motility of the synthetic AHL-deficient strain was significantly decreased compared to that of the wild-type strain, which was consistent with the biofilm formation results. EPSs are an important component of biofilms and provide the architectural form of biofilms and stabilize their 3-dimensional structure.[40] For example, EPS-producing mutants of *Mesorhizobium tianshanense* formed significantly less biofilm and displayed severely reduced nodulation capacity than wild-type bacteria.[42] In this research, we observed that biofilm formation, swimming motility, and EPS production synchronously declined in the *rosI* mutant strain compared to those in the wild-type strain, which coincided with the interrelationships between these phenotypes and QS regulation reported in previous studies.

A major goal of this research was to systematically analyze the structures and some physiological functions of QS in *R. oryzihabitans* M15. We now have evidence that a QS system is involved in the regulation of both growth- and colonization-related phenotypes and that multiple AHLs are produced by the bacteria. Overall, this study provides additional insights into rhizobia−rice plant interactions. The knowledge obtained from this study will be useful in advancing the research on the regulatory mechanism and signaling pathways of AHLs in rhizobia−rice interactions. Further studies are needed to identify the specific regulatory circuits of QS, the essential AHLs involved in a specific phenotype, and the essential target genes that lead to these responses.

https://doi.org/10.1021/acs.jafc.1c03895
J. Agric. Food Chem. 2021, 69, 9693−9705

■ ASSOCIATED CONTENT

Supporting Information

The Supporting Information is available free of charge at https://pubs.acs.org/doi/10.1021/acs.jafc.1c03895.

Bioreporter assay for AHLs production by *R. oryzihabitans* M15; production *m/z* values, retention time, and mass spectrometer parameters of AHL standards used in this study; structures of compounds **1**−**5**; phylogenetic tree of rosR against selected LuxR family transcriptional regulator from other *Rhizobium* species; PCR validation of *rosI* gene deletion; LC-MRM analysis of AHLs profiles in the wild type and *rosI* mutant strains of *R. oryzihabitans* M15 at 30 °C for 24 h (PDF)

■ AUTHOR INFORMATION

Corresponding Authors

Xiaoxia Zhang − *Key Laboratory of Microbial Resources Collection and Preservation, Ministry of Agriculture and Rural Affairs Institute of Agricultural Resources and Regional Planning, Chinese Academy of Agricultural Sciences, Beijing 100081, P. R. China*; Email: zhangxiaoxia@caas.cn

Guishan Zhang − *Key Laboratory of Microbial Resources Collection and Preservation, Ministry of Agriculture and Rural Affairs Institute of Agricultural Resources and Regional Planning, Chinese Academy of Agricultural Sciences, Beijing 100081, P. R. China*; Email: zhangguishan@caas.cn

Authors

Juanjuan Zhao − *Key Laboratory of Microbial Resources Collection and Preservation, Ministry of Agriculture and Rural Affairs Institute of Agricultural Resources and Regional Planning, Chinese Academy of Agricultural Sciences, Beijing 100081, P. R. China*; orcid.org/0000-0001-5048-5809

Guomin Ai − *State Key Laboratory of Microbial Resources, Institute of Microbiology, Chinese Academy of Sciences, Beijing 100080, P. R. China*

Sheng Yang − *Key Laboratory of Synthetic Biology, Institute of Plant Physiology and Ecology, Shanghai Institutes for Biological Sciences, Chinese Academy of Sciences, Shanghai 200032, P. R. China*; orcid.org/0000-0003-3742-9989

Complete contact information is available at: https://pubs.acs.org/10.1021/acs.jafc.1c03895

Notes

The authors declare no competing financial interest.

■ ACKNOWLEDGMENTS

This work was supported by the National Natural Science Foundation of China (NSFC nos. 31670113 and 31670005) and the Fundamental Research Funds for Central Non-profit Scientific Institution (No. 1610132019015).

■ REFERENCES

(1) Papenfort, K.; Bassler, B. L. Quorum sensing signal-response systems in gram-negative bacteria. *Nat. Rev. Microbiol.* **2016**, *14*, 576−588.

(2) Zhu, J.; Zhang, Y.; Deng, J.; Jiang, H.; Zhuang, L.; Ye, W.; Ma, J.; Jiang, J.; Feng, L. Diketopiperazines synthesis gene in *Shewanella baltica* and roles of diketopiperazines and resveratrol in quorum sensing. *J. Agric. Food Chem.* **2019**, *67*, 12013−12025.

(3) Wagner-Döbler, I.; Thiel, V.; Eberl, L.; Allgaier, M.; Bodor, A.; Meyer, S.; Ebner, S.; Hennig, A.; Pukall, R.; Schulz, S. Discovery of complex mixtures of novel long-chain quorum sensing signals in free-living and host-associated marine alphaproteobacteria. *ChemBioChem* **2005**, *6*, 2195−2206.

(4) Poole, P.; Ramachandran, V.; Terpolilli, J. Rhizobia: from saprophytes to endosymbionts. *Nat. Rev. Microbiol.* **2018**, *16*, 291−303.

(5) Calatrava-Morales, N.; McIntosh, M.; Soto, M. J. Regulation mediated by *N*-acyl homoserine lactone quorum sensing signals in the *Rhizobium*-legume symbiosis. *Genes* **2018**, *9*, No. 263.

(6) Schripsema, J.; de Rudder, K. E.; van Vliet, T. B.; Lankhorst, P. P.; de Vroom, E.; Kijne, J. W.; van Brussel, A. A. Bacteriocin small of *Rhizobium leguminosarum* belongs to the class of *N*-acyl-L-homoserine lactone molecules, known as autoinducers and as quorum sensing co-transcription factors. *J. Bacteriol.* **1996**, *178*, 366−371.

(7) Lithgow, J. K.; Wilkinson, A.; Hardman, A.; Rodelas, B.; Wisniewski-Dyé, F.; Williams, P.; Downie, J. A. The regulatory locus cinRI in *Rhizobium leguminosarum* controls a network of quorum-sensing loci. *Mol. Microbiol.* **2000**, *37*, 81−97.

(8) Daniels, R.; De Vos, D. E.; Desair, J.; Raedschelders, G.; Luyten, E.; Rosemeyer, V.; Verreth, C.; Schoeters, E.; Vanderleyden, J.; Michiels, J. The cin quorum sensing locus of *Rhizobium etli* CNPAF512 affects growth and symbiotic nitrogen fixation. *J. Biol. Chem.* **2002**, *277*, 462−468.

(9) Süle, S.; Cursino, L.; Zheng, D.; Hoch, H. C.; Burr, T. J. Surface motility and associated surfactant production in *Agrobacterium vitis*. *Lett. Appl. Microbiol.* **2009**, *49*, 596−601.

(10) Yang, M.; Sun, K.; Zhou, L.; Yang, R.; Zhong, Z.; Zhu, J. Functional analysis of three AHL autoinducer synthase genes in *Mesorhizobium loti* reveals the important role of quorum sensing in symbiotic nodulation. *Can. J. Microbiol.* **2009**, *55*, 210−214.

(11) Lugtenberg, B.; Kamilova, F. Plant-growth-promoting rhizobacteria. *Annu. Rev. Microbiol.* **2009**, *63*, 541−556.

(12) Zhao, J.; Zhao, X.; Wang, J.; Gong, Q.; Zhang, X.; Zhang, G. Isolation, identification and characterization of endophytic bacterium *Rhizobium oryzihabitans* sp. nov., from rice root with biotechnological potential in agriculture. *Microorganisms* **2020**, *8*, No. 608.

(13) Yuan, T.; Liu, L.; Huang, S.; Taher, A. H.; Tan, Z.; Wu, G.; Peng, G. *Rhizobium wuzhouense* sp. nov., isolated from roots of *Oryza officinalis*. *Int. J. Syst. Evol. Microbiol.* **2018**, *68*, 2918−2923.

(14) Glaeser, S. P.; Imani, J.; Al Ab Id, I.; Guo, H.; Kumar, N.; KäMpfer, P.; Hardt, M.; Blom, J.; Goesmann, A.; Rothballer, M.; et al. Non-pathogenic *Rhizobium radiobacter* F4 deploys plant beneficial activity independent of its host *Piriformospora indica*. *ISME J.* **2016**, *10*, 871−884.

(15) Alabid, I.; Hardt, M.; Imani, J.; Hartmann, A.; Rothballer, M.; Li, D.; Uhl, J.; Schmitt-Kopplin, P.; Glaeser, S.; Kogel, K.-H. The *N*-acyl homoserine-lactone depleted *Rhizobium radiobacter* mutant RrF4NM13 shows reduced growth-promoting and resistance-inducing activities in mono- and dicotyledonous plants. *J. Plant Disease Potect.* **2020**, *127*, 769−781.

(16) Zhang, X. X.; Gao, J. S.; Cao, Y. H.; Sheirdil, R. A.; Wang, X. C.; Zhang, L. *Rhizobium oryzicola* sp. nov., potential plant-growth-promoting endophytic bacteria isolated from rice roots. *Int. J. Syst. Evol. Microbiol.* **2015**, *65*, 2931−2936.

(17) Paphitou, N. I.; Rolston, K. V. Catheter-related bacteremia caused by *Agrobacterium radiobacter* in a cancer patient: case report and literature review. *Infection* **2003**, *31*, 421−424.

(18) Kutter, S.; Buhrdorf, R.; Haas, J.; Schneider-Brachert, W.; Haas, R.; Fischer, W. Protein subassemblies of the *Helicobacter pylori* Cag type IV secretion system revealed by localization and interaction studies. *J. Bacteriol.* **2008**, *190*, 2161−2171.

(19) Nester, E. W. *Agrobacterium*: nature's genetic engineer. *Front. Plant Sci.* **2014**, *5*, No. 730.

(20) Ohtani, I.; Kusumi, T.; Kashman, Y.; Kakisawa, H. A new aspect of the high-field NMR application of Mosher's method. The absolute configuration of marine triterpene sipholenol A. *J. Org. Chem.* **1991**, *56*, 4092−4096.

(21) O'Toole, G. A.; Kolter, R. Initiation of biofilm formation in *Pseudomonas fluorescens* WCS365 proceeds via multiple, convergent

signalling pathways: a genetic analysis. *Mol. Microbiol.* **1998**, *28*, 449−461.
(22) Rühmann, B.; Schmid, J.; Sieber, V. Methods to identify the unexplored diversity of microbial exopolysaccharides. *Front. Microbiol.* **2015**, *6*, No. 565.
(23) Nievas, F.; Bogino, P.; Sorroche, F.; Giordano, W. Detection, characterization, and biological effect of quorum-sensing signaling molecules in peanut-nodulating bradyrhizobia. *Sensors* **2012**, *12*, 2851−2873.
(24) Hao, G.; Burr, T. J. Regulation of long-chain *N*-acyl-homoserine lactones in *Agrobacterium vitis*. *J. Bacteriol.* **2006**, *188*, 2173−2183.
(25) Ravn, L.; Christensen, A. B.; Molin, S.; Givskov, M.; Gram, L. Methods for detecting acylated homoserine lactones produced by gram-negative bacteria and their application in studies of AHL-production kinetics. *J. Microbiol. Methods* **2001**, *44*, 239−251.
(26) Irie, Y.; Parsek, M. R. Quorum sensing and microbial biofilms. *Curr. Top. Microbiol. Immunol.* **2008**, *322*, 67−84.
(27) Ali, A.; Ayesha; Hameed, S.; Imran, A.; Iqbal, M.; Iqbal, J.; Oresnik, I. J. Functional characterization of a soybean growth stimulator *Bradyrhizobium* sp. strain SR-6 showing acylhomoserine lactone production. *FEMS Microbiol. Ecol.* **2016**, *92*, No. fiw115.
(28) Li, Y.; Gronquist, M. R.; Hao, G.; Holden, M. R.; Eberhard, A.; Scott, R. A.; Savka, M. A.; Szegedi, E.; Sule, S.; Burr, T. J. Chromosome and plasmid-encoded *N*-acyl homoserine lactones produced by *Agrobacterium vitis* wildtype and mutants that differ in their interactions with grape and tobacco. *Physiol. Mol. Plant Pathol.* **2005**, *67*, 284−290.
(29) Yue, Z.; Li, P.; Bin, L.; Huang, S.; Fu, F.; Yang, Z.; Qiu, B.; Tang, B. *N*-Acyl-homoserine lactone-mediated quorum sensing of aerobic granular sludge system in a continuous-flow membrane bioreactor. *Biochem. Eng J.* **2020**, No. 107801.
(30) Huang, S.; Zhang, H.; Ng, T.; Xu, B.; Shi, X.; Ng, H. Y. Analysis of *N*-Acy-L-homoserine lactones (AHLs) in wastewater treatment systems using SPE-LLE with LC-MS/MS. *Water Res.* **2020**, *177*, No. 115756.
(31) Liu, F.; Zhang, Y.; Liang, H.; Gao, D. Specific quorum sensing molecules of ammonia oxidizers and their role during ammonium metabolism in Zhalong wetland, China. *Sci Total Environ.* **2019**, *666*, 1106−1113.
(32) Gao, J.; Ma, A.; Zhuang, X.; Zhuang, G. An *N*-acyl homoserine lactone synthase in the ammonia-oxidizing bacterium *Nitrosospira multiformis*. *Appl. Environ. Microbiol.* **2014**, *80*, 951−958.
(33) Chen-Chen, M. A.; Jie, O. U.; Wang, J. Quantitation of quorum sensing signal molecules of *Pseudomonas* spp. isolated from meet. *Microbiol. China* 2013.
(34) Nieto-Peñalver, C. G.; Bertini, E. V.; de Figueroa, L. I. Identification of *N*-acyl homoserine lactones produced by *Gluconacetobacter diazotrophicus* PAL5 cultured in complex and synthetic media. *Arch. Microbiol.* **2012**, *194*, 615−622.
(35) Komiya-Ito, A.; Ito, T.; Yamanaka, A.; Okuda, K.; Yamada, S.; Kato, T. *N*-tetradecanoyl homoserine lactone, signaling compound for quorum sensing, inhibits *Porphyromonas gingivalis* growth. *Res. J. Microbiol.* **2010**, *5*, 1045−1051.
(36) Cataldi, T. R.; Bianco, G.; Abate, S. Profiling of *N*-acyl-homoserine lactones by liquid chromatography coupled with electrospray ionization and a hybrid quadrupole linear ion-trap and Fourier-transform ion-cyclotron-resonance mass spectrometry (LC-ESI-LTQ-FTICR-MS). *J. Mass Spectrom.* **2008**, *43*, 82−96.
(37) Filgueiras, L.; Silva, R.; Almeida, I.; Vidal, M.; Baldani, J. I.; Meneses, C. H. S. G. *Gluconacetobacter diazotrophicus* mitigates drought stress in *Oryza sativa* L. *Plant Soil.* **2020**, *451*, 57−73.
(38) Liu, X.; Zhang, K.; Liu, Y.; Zou, D.; Wang, D.; Xie, Z. Effects of calcium and signal sensing systems on *Azorhizobium caulinodans* biofilm formation and host colonization. *Front. Microbiol.* **2020**, *11*, No. 563367.
(39) Rinaudi, L.; Fujishige, N. A.; Hirsch, A. M.; Banchio, E.; Zorreguieta, A.; Giordano, W. Effects of nutritional and environmental conditions on *Sinorhizobium meliloti* biofilm formation. *Res. Microbiol.* **2006**, *157*, 867−875.
(40) Bogino, P. C.; Oliva Mde, L.; Sorroche, F. G.; Giordano, W. The role of bacterial biofilms and surface components in plant-bacterial associations. *Int. J. Mol. Sci.* **2013**, *14*, 15838−15859.
(41) Fujishige, N. A.; Kapadia, N. N.; De Hoff, P. L.; Hirsch, A. M. Investigations of *Rhizobium* biofilm formation. *FEMS Microbiol. Ecol.* **2006**, *56*, 195−206.
(42) Wang, P.; Zhong, Z.; Zhou, J.; Cai, T.; Zhu, J. Exopolysaccharide biosynthesis is important for *Mesorhizobium tianshanense*: plant host interaction. *Arch. Microbiol.* **2008**, *189*, 525−530.

https://doi.org/10.1021/acs.jafc.1c03895
J. Agric. Food Chem. 2021, 69, 9693−9705